Wind Evaporation on Wet Surfaces under Uncertainty Conditions

J.M. Gozálvez-Zafrilla[*,1], M.C. Leon-Hidalgo[1], A. Santafé-Moros[1], J.C. García-Díaz[2] and J. Lora-García[1]

[1]Institute for Industrial, Radiological and Environmental Safety (ISIRYM), Universidad Politécnica de Valencia, Spain

[2]Centro de Gestión de la Calidad y del Cambio (CGCC), Universidad Politécnica de Valencia, Spain

*Universidad Politécnica de Valencia (Dpto. Ing. Química y Nuclear, Ed. 5L). C/ Camino de Vera s/n. 46022 Valencia (Spain). E-mail: jmgz@iqn.upv.es

Abstract: Brine disposal from desalination plants placed in inland areas far from sea is an important problem. Evaporation ponds can be used for reducing the waste to solid state but they require huge amounts of land. Evaporation using arrays of wet surfaces can minimize the land requirements. One characteristic of the methods based on natural evaporation is the uncertainty associated to the influent variables (wind velocity, temperature and relative humidity) on the water evaporation rate.

To the aim of obtaining the performance of an experimental evaporation unit under random environmental conditions we have developed a model and then adjusted the mass transfer coefficient to experimental results. The uncertainty limits for the operation were obtained by a procedure based on the Monte Carlo method.

Keywords: Evaporation, Brine, Uncertainty, Monte Carlo.

1. Introduction

Desalination plants produce big amounts of brine. In coastal areas the logic management alternative is direct disposal into the sea with appropriate measures to reduce the environmental impact. However, in inland areas far from sea the disposal of the brines to land or water resources causes great environmental problems and the cost associated to brine management is very high [1].

Evaporation ponds can be used for reducing liquid waste to solid state [2]. However, its main drawback is the huge amounts of required land. Evaporation using arrays of wet surfaces (EAWS) can minimize land requirements. Several alternatives of this technique have been studied by Gilron et al. [3] and more recently by our research group [4].

In the most usual configuration of the dispositive, sheets of fabrics are disposed parallel in arrays. The fabrics are either partially submerged in a pond or wetted with brine poured from the top of the unit (Figure 1). The fabrics can be made of hygroscopic materials like cotton to facilitate capillarity, but other materials can also be used like polypropylene or PVC.

Besides the application to brine evaporation, the arrays of wet surfaces are used as humidifiers or to reduce the temperature of the air in few degrees. In this case, the devices used a fun to obtain a stable air velocity.
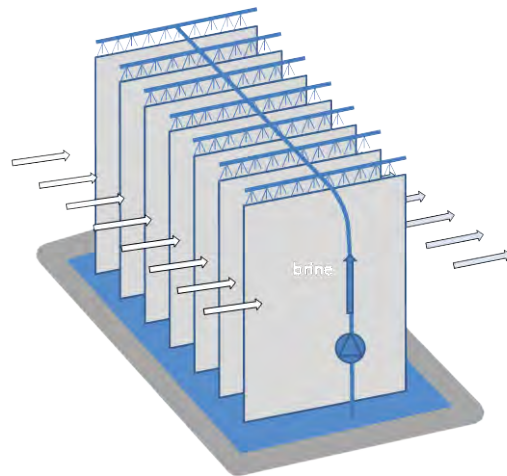
Figure 1. Scheme of a unit based in evaporation on arrays of wet surfaces (EAWS)

There are several factors that have influence on the performance of an EAWS device. The driving-force for evaporation is proportional to the difference of water partial pressures (between the bulk of the gas phase and the interface with the wet surface). In turn, partial water pressure of the air in contact with the wet surface depends on temperature. The specific evaporation rate (mass of water evaporated per unit of area and per unit

of time) is obtained by multiplying the driving-force by a mass transfer coefficient. This transfer coefficient strongly depends on the fluid dynamics conditions. Therefore, wind velocity, relative humidity and temperature are the relevant variables. In the laboratory, these variables can be controlled and the transfer coefficient can be obtained. In industrial devices based on forced ventilation, the hydrodynamic conditions and temperature can be controlled. However, when wind energy is used the ambient conditions have random behavior, that is, there is uncertainty in the influent input variables. Therefore, the performance of the EAWS device will also have random nature.

The work is divided into the following sections: First, we show how we modeled the performance of an EAWS device. Second, we explain how we fitted the values of the transport coefficient using experimental measures of the specific water evaporation rate. Third, the EAWS device is evaluated using the Monte Carlo method in a situation in which the probability distribution functions for the environmental conditions are known. Finally, we recapitulate the main conclusions obtained.

2. Modeling with COMSOL Multiphysics

The device that was modeled was a small commercial humidifier equipped with a fan able to achieve an air velocity of 1.7 m/s inside the channels. The device was adapted for the experiment. Feed solutions of 1000 ppm of NaCl were used to perform the experiments. Solution conductivity was continuously measured to calculate the evaporation rate by means of a salt balance between the state of the solution in each time and the feed solution (initial situation).

2.1 Domain geometry

The domain geometry was simplified in the following form: First, only one space between sheet elements was considered as identical fluid dynamic conditions were considered for each one of them. Second, the fluid domain was only half of a channel taking into account the symmetry of the fluid profile. Third, the fluid domain was reduced to a 2D geometry with the consideration of a wind velocity that was averaged for the system height. This is the strongest simplification as a non-uniform vertical velocity profile exists. However, this simplification was considered convenient to reduce the time of calculation per run as the Monte Carlo method is computationally intensive.

2.2 Physics and governing equations

Three physical modes of the Chemical Engineering Toolbox of COMSOL Multiphysics were used to solve the problem in steady-state mode: The "k-ε Turbulent mode" to solve the velocity profile of the system, the "Mass transport – Convection and Diffusion mode" to solve water diffusion from the wet surface to the air and the "Energy transport - Convection and Conduction mode" to solve the thermal effects.

Velocity profile

The "k-ε Turbulent mode" was selected because, except for very calmed weather conditions, the expected value of Reynolds number in the channels corresponds to turbulent conditions. This physics could be solved previously and separately from the others as air changes in humidity and temperature are small enough to not significantly affect viscosity and density of the gas mixture. Therefore, air properties correspondent to the input to the system were taken as constant in the fluid dynamic calculation.

Water transport

Water transport from the wet surface to the gas was modeled by a two steps mechanism. First laminar diffusion occurs in laminar boundary layer from the wet surface to the turbulent gas bulk (this was specified as a boundary condition). Second turbulent transport takes place in the gas domain and this is defined by the PDE of the "Convection and Diffusion mode".

The molar water flux due to laminar diffusion is given by (1):

$$J_w = k_C \cdot \left(C_{sat,w} - C_w \right) \qquad (1)$$

where $\qquad k_C = \dfrac{D_{w,air}}{\delta}$ $\qquad (2)$

The thickness of the boundary layer, δ, was considered as a parameter to be fitted from experimental data using the procedure defined in the section 3.

According to Treybal [5], under turbulent conditions the effective dispersion coefficient is a thousand times of the order of the laminar diffusion coefficient. For a gas, the eddy length scale for mass transport can be assumed to be the same as that of the momentum transport and energy transport.

The saturation pressure of brine solutions depends on concentration and can be calculated from polynomials fitted using experimental data [4]. However, as very diluted concentrations were used in the experiments the water vapor pressure (Pa) could be calculated using the correlation (3) for pure water [6].

$$P_{sat.w}(T) = \exp\left(A + \frac{B}{T} + C\ln(T) + D\,T^2\right)$$
$$A = 72.55 \qquad B = -7206.7 \tag{3}$$
$$C = -7.1385 \quad D = 4.046 \times 10^{-6}$$

Energy transport

The effect of the evaporation rate on the temperature profile of the fabrics was solved through an energetic balance considering the enthalpy associated to evaporation and the heat transfer due to difference of temperature. The water evaporation from the surface removes heat at the interface; therefore, a temperature decrease in the boundary is produced. This enthalpy flux, J_H, is given by (4)

$$J_H = J_w \cdot \lambda_w \cdot M_w \tag{4}$$

The latent heat of water, λ_w, was calculated using the correlation (5) for pure water [6]:

$$\lambda_w(T_r) = A \cdot (1 - T_r)^{B + C \cdot T_r + D \cdot T_r^2}$$
$$A = 2.8886 \times 10^6 \,\text{J/kg}$$
$$B = 0.3199 \quad C = -0.212 \quad D = 0.258 \tag{5}$$
$$\text{where} \quad T_r = \frac{T}{T_{crit,w}} \quad \text{with } T_{crit,w} = 647.35\,\text{K}$$

As a consequence of the temperature decrease on the surface, an enthalpy flux is established from the hotter surrounding gas to the interface. The turbulent enthalpy flux in the gas domain is calculated by the PDE system of the "Convection and Conduction mode".

2.3 Subdomain settings and boundary conditions

Figure 2 shows the fluid domain limited by four boundaries:
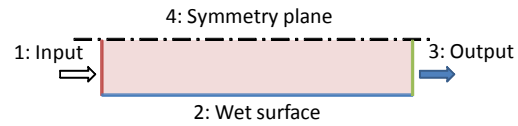
Figure 2. Fluid domain and limiting boundaries

The boundary conditions for each mode were the following:

Velocity profile

- Subdomain properties: Air properties temperature dependent (Material Library database of COMSOL)
- Boundaries:
  1. Normal inflow velocity, turbulent length scale = 0.08 L, turbulent intensity = 0.05.
  2. Logarithmic wall function with default wall offset.
  3. Outlet pressure = 101300 Pa.
  4. Symmetry boundary.

Water transport

- Subdomain properties: Turbulent diffusion coefficient.
- Boundaries:
  1. Water concentration in air $C_{w,1}$ in mol/m^3 (Eq 6).
  2. Inward flux by Eq. (1).
  3. Convective flux.
  4. Insulation/Symmetry boundary.

The input concentration was given by (6):

$$C_{w,1} = \frac{P_{w,1}}{R_G \cdot T_1} \tag{6}$$

where partial water pressure at the input was calculated from relative humidity and absolute temperature by means of equation (7):

$$P_{w,1} = \frac{RH_1(\%)}{100} \times P_{sat,w}(T_1) \qquad (7)$$

Energy transport

- Subdomain properties: Thermal conductivity.
- Boundaries:
  1. Air temperature, T_1 in K.
  2. Inward heat flux by Eq. (4).
  3. Convective flux.
  4. Thermal insulation.

2.4 Meshing

The mesh used had 100 elements in boundary 4 (Figure 3). A more refined mesh was used near to the evaporation surface where higher gradients were expected.

Figure 3. Mesh used

2.5 Solver used

The direct solver UMFPACK was used to solve the problem. First, the solution was obtained for the k-ε Turbulence Model with air properties at the input temperature. Afterwards, the solution was obtained incorporating the other modes.

3. Fitting to experimental results

To find the transport coefficient, k_C, that correspond to a specific-evaporation-rate value, we applied an iteration procedure based in quadratic interpolation that we have previously used [7]. The COMSOL post-processing mode was used to obtain the average specific evaporation rate (mg·m^{-2}·s^{-1}) by integrating the flux and further dividing for the channel length. An experiment at T = 20 °C, relative humidity of 45% and air velocity of 1.7 m/s obtained a stable evaporation rate of 74.4 mg·m^{-2}·s^{-1}. For this value, the fitting procedure yielded to the value $k_C = 7.8 \times 10^{-3}$ m/s.

As previously stated, the air properties are not significantly modified for changes in temperature and relative humidity. Consequently, the main effects on the transport coefficient are those of the velocity. The Sherwood number that includes the transport coefficient depends on the Reynolds number to the power of 0.8 [5]. Therefore, Equation (8) was used to estimate the value of the transport coefficient for other velocities using as reference value the one that was obtained from the experiment.

$$k_C(v) = k_{C,ref} \cdot \left(\frac{v}{v_{ref}} \right)^{0.8} \qquad (8)$$

4. Uncertainty study by the Monte Carlo method

As an example of determination of the uncertainty associated to weather conditions, we simulated the performance of the modeled device for a specific location (Valencia, in the Mediterranean coast of Spain) and weather period (month of May). The data (620 observations) were compiled during the period 2005-2010 [8]. The influent variables on the water evaporation rate that are going to be studied are wind velocity, temperature and relative humidity. Wind direction was not taken into account as we consider that the system could be oriented in the wind direction.

The procedure of model analysis by the Monte Carlo propagation method implies to generate a number of random combinations of the input variables [9]. Then, the solutions for each combination are computed. The set of values that has been obtained can be used to estimate the statistical properties of the output. Typically, fitted parametric distributions of the data are used to generate the combinations. For example, the data of wind velocity and temperature can be fitted to the Weibull and the normal distribution respectively (Figures 4 and 5). However, the distribution of relative humidity data does not correspond to any usual parametric distribution (Figure 6). Besides, relative humidity is somehow correlated with temperature. Therefore, to generate the input data set in this case the data were pooled by

random choice from the extensive database taking together the wind velocity, the relative humidity and the temperature corresponding to each selected observation.
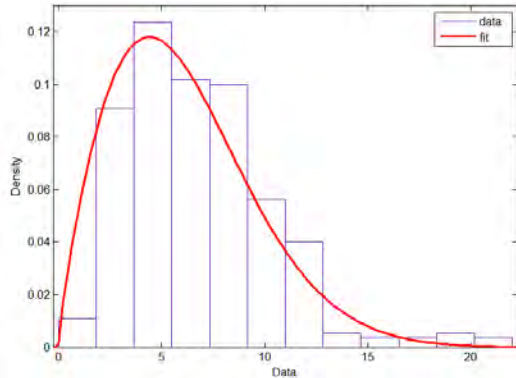
Figure 4. Probability distribution of wind velocity data (km/h) and fitting to a Weibull distribution
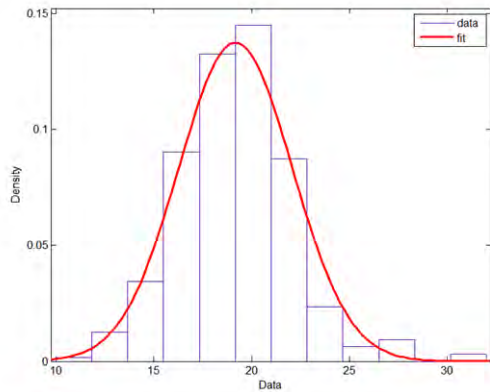
Figure 5. Probability distribution of temperature data (°C) and fitting to a normal distribution
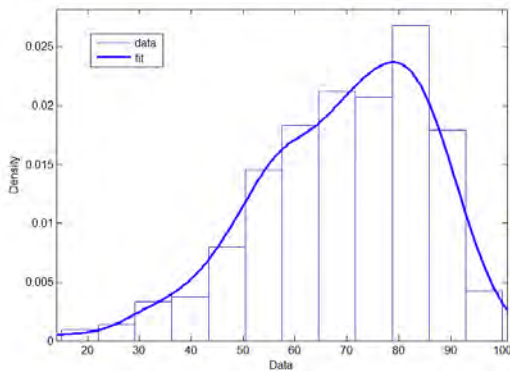
Figure 6. Probability distribution of relative humidity data (%) and fitting to a non-parametric distribution

To determine the lower uncertainty bound, the criterion used to determine the number of Monte Carlo runs was that the response variable had to be comprised between the upper and lower boundary margins with a probability content α = 95% and a confidence level β = 95%. According to Wilks' formula (9) for one-sided tolerance limits the necessary number of model runs is 59 [10].

$$N = \frac{\ln(1-\beta)}{\ln(\alpha)} \qquad (9)$$

To minimize the computation time and facilitate convergence, the combinations generated for the Monte Carlo Method were sorted in a list according to increasing partial water pressure. Then a script was used to sequentially call COMSOL to calculate each solution using as initial guess the solution of the previously calculated run of the list.

Figure 7 shows the histogram of the calculated data of evaporation rate and Table 2 their statistical properties. The wide distribution of the results indicates that there is high uncertainty for the outside operation of the device. Regarding to the median value, the system would be working half of the days with an evaporation rate greater than 28.9 mg·m^{-2}·s^{-1}, so there would be a low performance during the rest of the month. The lower bound indicates that 95% of the time the device will be working with an evaporation rate greater than 4.4 mg·m^{-2}·s^{-1}, which is a very low value.
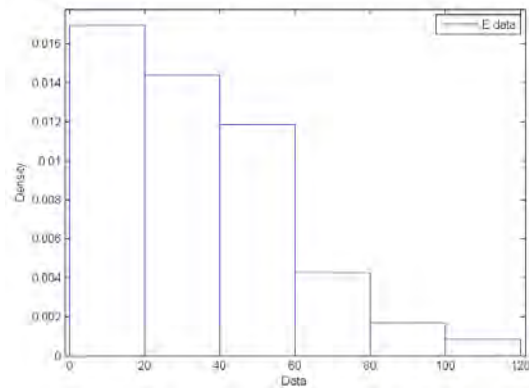
Figure 7. Probability distribution of the evaporation rate (mg·m^{-2}·s^{-1})

Table 2: Statistic properties of the distribution obtained for the specific evaporation rate (mg·m^{-2}·s^{-1}).

Statistic parameter	Value
Mean	34.9
Median	28.9
Lower bound	4.4

The Monte Carlo propagation method was also used to perform a sensitivity analysis of the effects of each source of uncertainty on the water evaporation rate (Figures 8 to 10). Surprisingly the temperature was not significantly correlated to the evaporation rate as a linear rank correlations of $r = -0.15$ was obtained. On the contrary, for relative humidity and wind velocity values of $r = -0.68$ and $r = +0.59$ were obtained respectively that agree with the physics of the phenomena. The linear rank correlation obtained for temperature can be explained by the fact that for a coastal region high temperature is usually associated to high humidity.

5. Conclusions

A simplified model of a device based on wet surfaces was developed using COMSOL Multiphysics and their parameters fitted to experimental data.

The application of The Monte Carlo method was useful to obtain the uncertainty limits for the device operating at a specific month of the year in a specific location. The results are important to determine a safe operating capacity for the device.
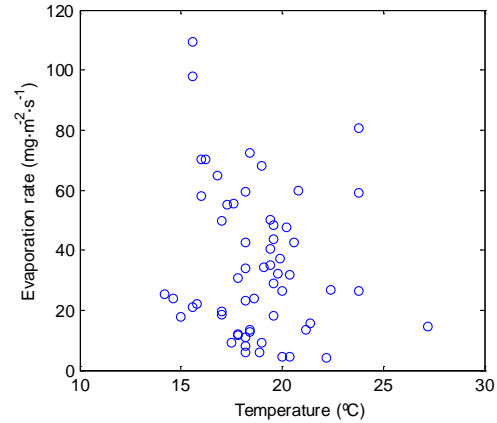
Figure 8. Specific evaporation rate (mg·m^{-2}·s^{-1}) vs. temperature (°C)
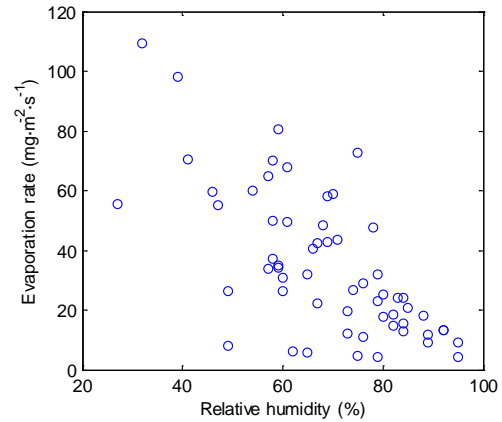
Figure 9. Specific evaporation rate (mg·m^{-2}·s^{-1}) vs. relative humidity (%)
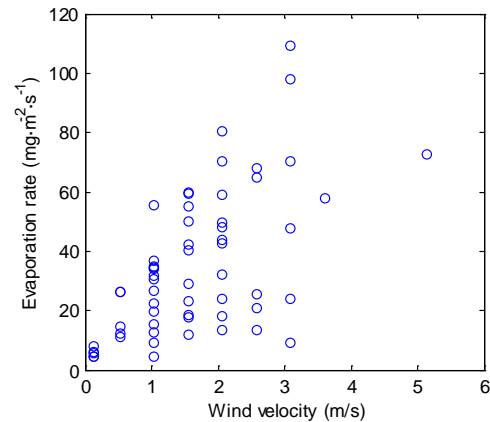
Figure 10. Specific evaporation rate (mg·m^{-2}·s^{-1}) vs. wind velocity (m/s)

6. List of variables

A, B, C, D correlation coefficients
$D_{w,air}$ diffusivity of water in air, $m^2 \cdot s^{-1}$
J_H heat flux, $J \cdot m^{-2} \cdot s^{-1}$
J_w molar water flux, $mol \cdot m^{-2} \cdot s^{-1}$
k_C laminar transport coefficient, $m \cdot s^{-1}$
M_w molecular mass of water, $0.018 \ kg \cdot mol^{-1}$
$P_{sat,w}$ saturation pressure of water, Pa
P_w partial pressure of water, Pa
R_G gas perfect constant, $8.314 \ J \cdot mol^{-1} \cdot K^{-1}$
RH relative humidity, %
T temperature, K
T_{crit} critical temperature, K
T_r reduced temperature, adim.
v velocity, m/s

α probability content
β confidence level
δ thickness of boundary layer, m
λ latent heat of water evaporation, $J \cdot mol^{-1}$

7. References

1. M. Wilf, M. Mickley et al.; *The Guidebook to Membrane Desalination Technology: Reverse Osmosis, Nanofiltration and Hybrid Systems Process, Design, Applications and Economics*, 375-389. Balaban desalination publications, Italy (2007)

3. M. Ahmed, W.H. Shayya, D. Hoey, A. Mahendran, R. Morris, J. A1-Handaly; Use of evaporation ponds for brine disposal in desalination plants, *Desalination*, **130**, 155-168 (2000)

3. J. Gilron; Y. Folkman, R. Savliev, M. Waisman, O. Kedem; WAIV - Wind aided intensified evaporation for reduction of desalination brine volume, *Desalination*, **158**, 205-214 (2003)

4. M.C. Leon-Hidalgo, J.M. Gozalvez-Zafrilla, J. Lora-Garcia et al.; Study of the vapor pressure of saturated salt solutions and their influence on evaporation rate at room temperature, *Desalination and Water Treatment*, **7**, 111-118 (2009)

5. R.H. Treybal. Mass Transfer Operations, 2nd ed., 50-70

6. CHEMCAD 6.0 ® Databank.

7. J.M. Gozálvez-Zafrilla, J.M. Serra, A. Santafé-Moros; Modeling of High-Temperature Ceramic Membranes for Oxygen Separation, *Proceedings of the European COMSOL Conference*, Milano, Italy (2009)

8. http://www.meteovalencia.org

9. C.E. Papadopoulos, H. Yeung; Uncertainty estimation and Monte Carlo simulation method, *Flow Measurement and Instrumentation*, 12, 291–298 (2001)

10. S.S. Wilks; Determination of sample sizes for setting tolerance limits, *Annals of Mathematical Statistics*, 1, 91–96 (1941)

8. Acknowledgements